# Energy Transfer and Exciton Annihilation in the B800−850 Antenna Complex of the Photosynthetic Purple Bacterium *Rhodopseudomonas acidophila* (Strain 10050). A Femtosecond Transient Absorption Study

**Ying-Zhong Ma,[†] Richard J. Cogdell,[‡] and Tomas Gillbro*[,†]**

*Department of Physical Chemistry, University of Umeå, S-901 87 Umeå, Sweden, and Division of Biochemistry and Molecular Biology, University of Glasgow, Glasgow G12 8QQ, U.K.*

*Received: August 14, 1996; In Final Form: November 11, 1996*[⊗]

Excitation energy transfer and exciton annihilation in the isolated B800−850 antenna complex from the purple bacterium *Rhodopseudomans acidophila* (strain 10050) were studied by one-color transient absorption experiments with a typical pulse length of 50 fs at room temperature and 77 K. The anisotropy kinetics observed within the B800 band are clearly wavelength dependent, indicating that the B800 ↔ B800 energy transfer or excitonic relaxation processes are wavelength dependent. The depolarization times found at room temperature were 400 fs at 790 nm, 820 fs at 800 nm, and 360 fs at 810 nm. A faster depolarization time of 240 fs was obtained at 801 nm at 77 K, which is suggested to originate from excitonic relaxation. Energy transfer from the B800 to the B850 occurs in ∼0.8 ps at room temperature and ∼1.30 ps at 77 K. The kinetics obtained within the B800 band were observed for the first time to exhibit a dramatic dependence on the excitation intensity. When the excitation intensity is higher than $1.09 \times 10^{14}$ photons pulse$^{-1}$ cm$^{-2}$, the transient absorption kinetics after ∼3 ps are dominated by a long-lived bleaching. However, in contrast, a slowly recovering excited-state absorption was found to be dominant at lower pump intensities. This intensity dependence is attributed to the variation of the population distribution between the lowest and next higher lying excitonic levels of the B850 ring, a result of exciton annihilation in the lowest-state, following the rapid energy transfer from the B800 to the B850 band and subsequent fast excitonic relaxation within the excitonic manifold of the B850 ring. The time constant for this annihilation process was found to be ∼1 ps. Excitonic calculations indicate that several high-lying excitonic states show good spectral overlap with the B800 band, and thus, they could serve as excellent acceptors for the energy transfer from B800 to B850.

## I. Introduction

The light-harvesting system of photosynthetic purple bacteria generally possesses a peripheral light-harvesting antenna (LH2) and a core antenna (LH1).[1,2] The latter surrounds the reaction center where a charge separation occurs, producing energy for subsequent photochemical reactions. Different types of LH2 bacteriochlorophyll−protein complexes have been found, e.g., B800−820, B800−830, and B800−850 complexes, etc. The variation of the longer wavelength absorption band position depends on the species and strain of bacteria, as well as the growth conditions.[3] For example, the purple bacterium of *Rhodopseudomonas acidophila* (*Rps. acidophila*) is capable of synthesizing either B800−820 or/and B800−850 types of complexes, depending on the strain, light intensity, and temperature. Among the three known wild types of *Rps. acidophila*, i.e., strains 7050, 7750, and 10050, it was found that only strain 10050 can synthesize the pure B800−850 complex.[4]

The newly available structure of the LH2 complex from *Rps. acidophila* strain 10050 at a resolution of 2.5 Å[5] has provided an excellent opportunity for a detailed study of excitation energy transfer in the LH2 antenna complexes of purple bacteria. For this specific LH2 complex the BChl *a* molecules form two ring structures. The 800 nm absorbing BChl *a* molecules are located between the $\beta$-apoproteins, with their bacteriochlorin planes parallel to the presumed cytoplasmic membrane surface, and the closest distance between the central Mg atoms is 21 Å. The 850 nm absorbing BChl *a* pigments are positioned between the inner and outer protein walls formed by nine $\alpha$- and $\beta$-apoproteins arranged in a complete ring of 18 interacting BChl *a* molecules with the bacteriochlorin planes parallel to the membrane normal. These 18 molecules are organized in nine identical protomers, where each protomer contains two B850 BChl *a* pigments. The Mg···Mg distance between the two BChl *a* molecules within the same protomer was found to be 8.7 Å, while it is 9.7 Å between adjacent protomers. The distance between the central Mg atoms of the closest B800 and B850 molecules is 17.6 Å.

Thus far, excitation energy transfer between the BChl *a* molecules in various B800−850 antenna complexes from different bacterial species have been extensively studied by steady-state, frequency- and time-domain optical spectroscopy techniques. For a detailed description, we refer to a recent review.[1] The interband transfer time from B800 to B850 has been determined to be 0.70−0.8 ps at room temperature, and it slows down to 2.4 ps at 77 K.[6−11] Very similar transfer times were also found by hole-burning experiments at even lower temperatures (1.2 and 4.2 K).[12−15] A considerably faster transfer time was observed at 77 K recently by Monshouwer et al.[16] under a low-intensity pump−probe measurement. Thus, a transfer time of 1.2 ± 0.1 ps was found in the B800−850 complex of *Rb. sphaeroides* at 77 K, and the slow decay lifetime, observed under high excitation intensity, was suggested to be a result of photodamage to the complex. Similar shorter time constants were found in our recent measurements on the B800−820 antenna complex from *Rps. acidophila* (strain 7750).[17] Besides the discrepancy of this interband transfer time

[†] University of Umeå.
[‡] University of Glasgow.
* Corresponding author. Telephone: 46-90-16-53-68. Fax: 46-90-16-77-79, E-mail: tomas.gillbro@chem.umu.se.
[⊗] Abstract published in *Advance ACS Abstracts,* December 15, 1996.

S1089-5647(96)02470-4 CCC: $14.00 

at low temperatures, a fundamental question concerning the acceptor state of the B850 band remains unsolved. Two possible candidates that have been suggested so far are either a vibrational mode of the B850 band in a monomeric model[12,14] or an upper excitonic state for the strong coupling case.[10]

In this paper, we describe the results of a direct femtosecond time-resolved study on the B800−850 complex isolated from *Rps. acidophila* (strain 10050). The experiments were performed at several excitation and detection wavelengths within the B800 band as well as at the blue edge of the B850 band, using the so-called one-color transient absorption technique with typical pulse lengths of 50 fs. Remarkable pump intensity dependent transient absorption kinetics were observed for the first time within the B800 band. The dramatic change of the kinetics under high pump intensity is attributed to the variation of the population distribution between the lowest- and the next higher-lying excitonic levels of the B850 ring arising from exciton annihilation in the lowest-lying excitonic state. The higher-lying excitonic states are proposed to be the acceptor states for the interband transfer. The interband transfer takes ∼0.80 ps at room temperature and ∼1.30 ps at 77 K. Analysis of the depolarization kinetics obtained, in combination with the newly determined LH2 structure, gives new insight into the intra-B800 band energy transfer processes.

## II. Materials and Methods

The B800−850 complex was prepared as described elsewhere[18] and stored in a freezer (less than −20 °C) until use. The sample was resuspended in 50 mM Tris-HCl (pH 8.0) to give a maximum absorbance of about 0.5 in a 1 mm glass cuvette for the femtosecond pump−probe measurements. A rotating cell of 1 mm path length with glass windows was also used in some room temperature experiments in order to check for any possible sample damage due to laser illumination during the measurement. Since no observable difference was identified for the static and rotating samples, we will therefore not specify the sample state for the kinetics reported in this paper. Low-temperature experiments were performed using an Oxford Instruments liquid-$N_2$ cryostat. To obtain a good quality glass upon freezing, the sample was mixed to about 60% (v/v) glycerol and a maximum optical density of about 0.5 in a 1.0 mm glass cuvette was used.

The steady-state fluorescence emission spectrum was measured with a SPEX Fluorolog 112 fluorometer equipped with a Hamamatsu R928 red-sensitive multialkali photomultiplier. The emission polarizer was set to the magic angle (54.7°) with respect to the excitation polarizer. Excitation was at 591 nm and the bandwidths for the excitation and emission monochromators were 3.7 and 3.6 nm, respectively.

The femtosecond absorption measurements were performed using the one-color pump−probe technique. A mode-locked femtosecond Ti:sapphire laser (Spectra Physics Tsunami) pumped by all lines of an $Ar^+$ laser was used to produce near-infrared femtosecond pulses with a typical duration of approximately 80 fs at a repetition rate of 82 MHz. A low repetition rate in the range 0.4 kHz to 4 MHz was achieved by use of a pulse picker (Spectra Physics Model 3980) containing an optoacoustic crystal to avoid long-lived photoproducts distorting the real kinetics. Measurements reported in this paper were carried out at two repetition rates, 80 and 400 kHz, and again, no detectable change of the kinetics was found between these two repetition rates. A dual SF10 prism pulse compressor installed after the pulse picker made it possible to obtain transform-limited pulses as short as 50 fs. After the prism compressor the light was directed into a standard noncollinear pump−probe setup, where

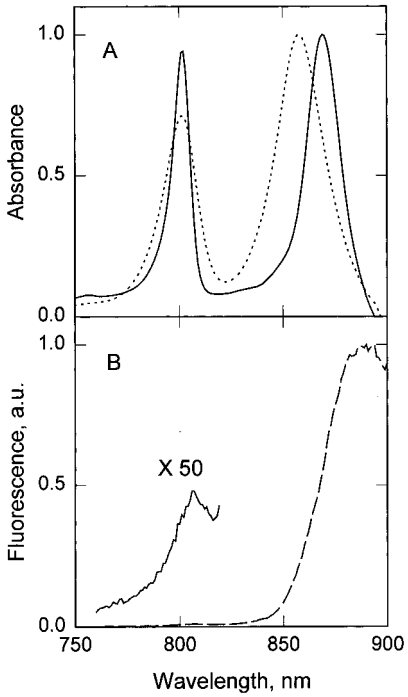


**Figure 1.** (A) NIR steady-state absorption spectra of the B800−850 complex from *Rps. acidophila* strain 10050 at both room temperature (dotted line) and 77 K (solid line). These two spectra have been normalized at the maxima of the B850 band. (B) Fluorescence emission spectrum at room temperature upon excitation at 591 nm. The emission from the B800 band has been expanded by a factor of 50 for the sake of clarity.

the pulse train was divided into pump and probe beams with an intensity ratio of 20:1. The maximum available pump power was less than 0.75 nJ/pulse with a beam diameter of about 40 $\mu$m in the beam overlap region. This corresponds to a maximum photon flux of $3.0 \times 10^9$ photons pulse$^{-1}$, and thus, approximately 15% of the B800 molecules were excited, estimated using an extinction coefficient of $213 \pm 28$ mM$^{-1}$ for B800.[19] This pump power was further attenuated with neutral density filters in order to obtain the decay kinetics under different pump intensities, as well as kinetics free of excitation annihilation effects. The excitation beam was linearly polarized (vertically) using a Berek's polarization compensator (Model 5540, New Focus). The probe pulses were delayed with respect to the pump pulses by a computer-controlled stepping-motor-driven optical delay line, and its polarization was varied among parallel, perpendicular, and the magic angle (54.7°) with respect to the pump pulse polarization by using a Soleil−Babinet compensator. The pump beam was modulated at a frequency of ∼1 kHz, and the integrated probe signal was measured with an infrared sensitive photodiode, and the signals were registered by a lock-in amplifier interfaced with a personal computer. The autocorrelation function of the pump and probe pulses was recorded by simply replacing the sample cell by a thin BBO crystal.

The whole system was carefully tested before measurements were made by using the laser dye IR140 in methanol solution. This system has a constant anisotropy of 0.4 for at least several tens of picoseconds as shown previously.[20]

## III. Results

**A. Steady-State Absorption and Fluorescence Spectra**. Figure 1A shows the NIR steady-state absorption spectra of the B800−850 complex at room temperature and at 77 K. The absorption maxima of the B800 and B850 bands are located at 801 and 858 nm at room temperature. These two absorption

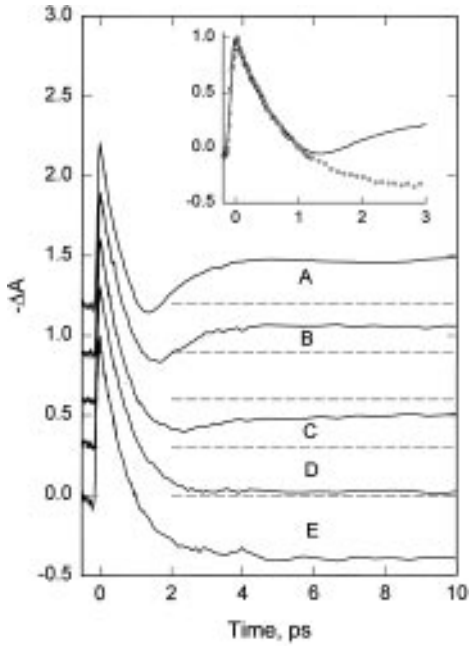


**Figure 2.** Isotropic decay kinetics at 800 nm at room temperature measured under different pump intensities: (A) $1.20 \times 10^{14}$, (B) $1.09 \times 10^{14}$, (C) $6.0 \times 10^{13}$, (D) $3.79 \times 10^{13}$, and (E) $2.40 \times 10^{13}$ photons pulse$^{-1}$ cm$^{-2}$. The kinetics have been normalized by the transient ansorbances at time zero and vertically offset for the sake of clarity. The horizontal dashed lines show the base line for each kinetic trace. The insert shows the kinetics obtained at the two extreme pump intensities, $1.20 \times 10^{14}$ photons pulse$^{-1}$ cm$^{-2}$ (solid line) and $2.40 \times 10^{13}$ photons pulse$^{-1}$ cm$^{-2}$ (open circles), on a short time scale. The initial fast recoveries of these two kinetics have comparable lifetimes.

bands appear narrower at 77 K with maxima located at 802 and 869 nm. Thus, only the B850 band shows a significant red shift upon a decrease of the temperature to 77 K. The fluorescence emission spectrum at room temperature exhibits two bands with maxima located at ca. 806 and 890 nm, as shown in Figure 1B, attributed to B800 and B850 emissions. The peak intensity of this short wavelength band is approximately 2 orders of magnitude smaller than the long wavelength band.

**B. Intensity Dependence of the Transient Absorption Kinetics**. A significant finding of our present experiments is the dramatic intensity dependence of the transient absorption kinetics measured within the B800 band at room temperature. Figure 2 shows the intensity dependence of the normalized isotropic kinetics measured at 800 nm using neutral density filters to vary the pump intensities. At high pump intensity ($1.20 \times 10^{14}$ photons pulse$^{-1}$ cm$^{-2}$, plot A), the kinetics initially exhibit a fast recovery from the ground state photobleaching and/or stimulated emission. It further develops into a small positive transient absorption due to excited state absorption (ESA) of the B850, and finally, it turns again to give a transient depletion, which recovers very slowly (not shown). As the pump intensity is decreased from $1.20 \times 10^{14}$ to $1.09 \times 10^{14}$ photons pulse$^{-1}$ cm$^{-2}$ (plot B), the turning behavior of the transient absorption kinetics is still present, but the ratio of the long time bleaching signal to the transient absorption at time zero clearly decreases. When the pump intensity is decreased to $6.0 \times 10^{13}$ photons pulse$^{-1}$ cm$^{-2}$ (plot C), the turning pattern can still be seen but the long-lived signal shows only an ESA. On further decrease of the intensity to $3.79 \times 10^{13}$ (plot D) and $2.40 \times 10^{13}$ photons pulse$^{-1}$ cm$^{-2}$ (plot E), only an increase of the transient absorption, due to the ESA of B850, is observed at longer times and no turning point appears. This is the normal type of transient absorption kinetics that have been commonly found in the B800 bands of different LH2 light-harvesting antenna of various purple bacteria.[6−8,16,17] It should be noted that even for the nonturning shape kinetics (D and E), there is still a minor difference in the relative amplitudes of the ESA component; it is larger at the lower pump intensity used.

The complicated shape of the kinetics obtained under high pump intensity conditions makes it very difficult to perform an accurate deconvolution fitting. However, the initial fast recovery lifetime in the turning type of kinetics is identical with that determined for the kinetics showing no turning feature (obtained at the lowest intensity), and therefore, it should represent the same dynamic process (interband energy transfer as discussed in section IV.B). This can be clearly seen in the insert of Figure 2, where the normalized kinetics obtained at the highest (A) and lowest (E) pump intensities are plotted together. To determine the time constant for the formation of the transient depletion observed at later times for the kinetics measured under higher intensities, we have to employ a separate fitting procedure, taking the sudden turning point as the temporal separation point. The time constant was found to be ∼1 ps at the pump intensities $1.20 \times 10^{14}$ and $1.09 \times 10^{14}$ photons pulse$^{-1}$ cm$^{-2}$, respectively. As the pump intensity is further decreased to $6.0 \times 10^{13}$ photons pulse$^{-1}$ cm$^{-2}$, an additional minor rise component is required to give a good fit and the lifetime was found to be 5.1 ps with a relative amplitude of less than 20%. However, the low-level signal at this pump intensity results in a greater uncertainty in this lifetime. The 1 ps lifetime also seems to be polarization independent. Deconvolution fitting, by the same procedure, for the parallel and perpendicular polarized kinetics obtained at 790, 800, and 810 nm gave the same time constants (not shown).

We want to point out that the kinetics are very sensitive to the pump intensity and that the dramatic changes observed occur for an intensity variation of only a factor of 3! Such an intensity dependence, to our knowledge, has not been observed before in other LH2 antenna complexes from different bacterial species.[6−8,16] An additional feature of this intensity dependence is that the time constants are very similar (∼1 ps) and seem to be independent of the excitation intensity. Thus, there is a clear distinction from the phenomena of excitation annihilation characterized by the biexcitation decay rate constant $\gamma_2$, where obvious intensity dependent lifetimes were observed.[2,21]

**C. Isotropic Transient Absorption Kinetics Measured at Low Pump Intensity**. In view of the remarkable pump intensity dependence of the transient absorption kinetics observed within the B800 band and the difficulty in their optimal deconvolution fitting, special care was taken to obtain kinetics free of this turning feature. These type of kinetics were obtained by reducing the pump intensity using neutral intensity filters. The nonturning type of kinetics are important for the accurate determination of the energy transfer time constants. Three kinetics were measured at 790, 800 and 810 nm, respectively, under low pump intensity, and all of them were initiated with a fast recovery as a result of photobleaching and/or stimulated emission, followed by ESA of B850 molecules. This is a result of the spectral overlap of the ground-state absorption (GSA) of B800 BChl *a* molecules and the ESA of B850 pigments. All the isotropic decay kinetics can be fitted well with a two-exponential decay function, and the fitting parameters are summarized in Table 1. The fast decay component has a lifetime of ∼0.8 ps at room temperature and seems to be very weakly wavelength dependent in the range 790−810 nm as shown in Figure 3. The slow component represents the decay of the ESA of the B850 band. These lifetimes were not accurately determined because of the shorter scan range used in the present measurements (<100 ps). The decay kinetics

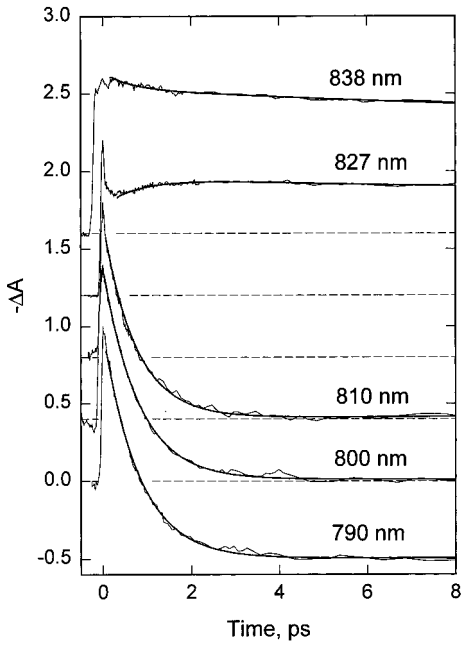


**Figure 3.** Isotropic decay kinetics measured at room temperature and at 790, 800, 810, 827, and 838 nm. The thin line in each case represents the experimental curve, and the thick line is the corresponding best fit with the optimized parameters given in Table 1. The kinetics have been normalized by the transient absorbance at time zero and offset for clarity with the dashed lines indicating the base lines of the kinetics.

**TABLE 1: Decay Lifetimes and Relative Amplitudes of the Isotropic Transient Absorption Kinetics at Different Wavelengths for B800−850 Complex from *Rps. acidophila* at Room Temperature (RT is ∼298 K) and 77 K**

| $\lambda$ (nm) | $T$ (K) | $\tau_1$ (ps) | $A_1$ | $\tau_2$ (ps) | $A_2$ | $\tau_3$ (ps) | $A_3$ |
|---|---|---|---|---|---|---|---|
| 790 | RT | | | 0.80 | 1.0 | 810 | −0.34 |
| 800 | RT | | | 0.79 | 1.0 | 950 | −0.23 |
| 810 | RT | | | 0.74 | 1.0 | 320 | −0.31 |
| 827 | RT | 0.89 | −0.20 | 3.50 | 0.09 | 430 | 0.91 |
| 838 | RT | 0.57 | 0.09 | 15.7 | 0.22 | 660 | 0.69 |
| 788 | 77 | 0.043 | 0.69 | 0.71 | 0.31 | 300 | −0.14 |
| 801 | 77 | 0.036 | 0.42 | 1.30 | 0.58 | 130 | −0.18 |

measured at longer wavelengths are different, and no ESA is seen at 827 or 838 nm (Figure 3). Instead, a slow and dominant bleaching component was found with a long lifetime (see Table 1). A weak depletion feature (like a "rise" in the $-\Delta A$) was also seen at 827 nm with a lifetime of 0.89 ps, a region between the B800 and the B850 bands, and thus, both the B800 and B850 BChl *a* can be excited. The kinetics obtained at 838 nm, at the blue edge of the B850 band, are free of the "rise" feature, and instead, a fast recovery component with a lifetime of approximately 0.57 ps and an intermediate one of ∼16 ps were resolved but with lower amplitudes in addition to the slow dominant component (see Table 1).

When the temperature is decreased to 77 K, the isotropic kinetics also appear to be wavelength dependent, as seen at 788 and 801 nm (Figure 4). Both sets of kinetics can be fitted well with a three-exponential decay function, but only the intermediate component ($\tau_2$) can be accurately determined because of the presence of the coherent spike as well as the short scan range used. As shown in Table 1, the decay lifetime is 0.71 ps at 788 nm and 1.30 ps at 801 nm. In comparison to the corresponding value obtained at room temperature, the lifetime obtained around 800 nm is only slightly longer.

**D. Time-Resolved Anisotropy**. The presence of ESA in the kinetics observed within the B800 band, at both room temperature (under low pump intensity) and 77 K, makes it very difficult to perform direct calculations of the anisotropy decay

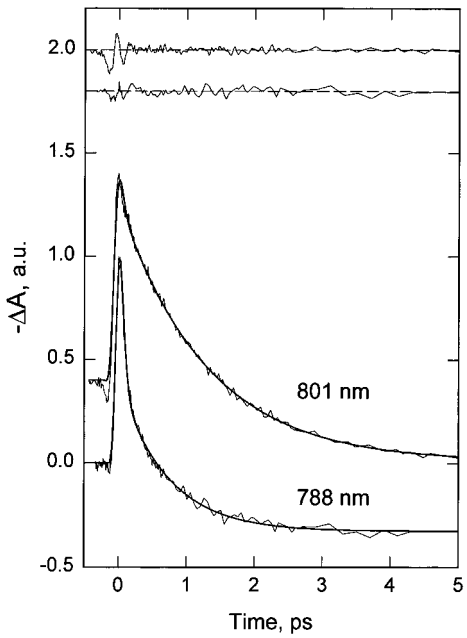


**Figure 4.** Isotropic decay kinetics measured at 77 K and at 788 and 801 nm. The thin line in each case represents the experimental curve, and the thick line is the best fit. The kinetics have been normalized by the transient absorbance at time zero and offset for clarity. The insert shows the corresponding residuals for the fits of the kinetics.

from the raw data. This is probably due to considerably different transition dipole orientations for the GSA and ESA. Moreover, there would be a break point in the anisotropy decay, which corresponds to the zero value of the isotropic $\Delta A$. Therefore, we have to calculate the anisotropy decays by an indirect method. Fortunately, the signals from the photobleaching and the ESA clearly have different origins, B800 and B850, respectively, and thus, in principle they could be separated from each other by data analysis. Such a method begins with the separate deconvolution fitting of the kinetics measured at parallel and perpendicular polarizations. As for the isotropic kinetics fits, all the parallel and perpendicular kinetics could be fitted well by using a two- or three-exponential decay function with a slow component representing the ESA recovery. The part due to the ESA was subtracted from the measured parallel and perpendicular kinetics according to the lifetime and amplitude obtained from the best fit, and thus, the resulting kinetics will decay to zero with time constants depending on the wavelength as well as temperature. These corrected kinetics were then used to calculate the anisotropy decay using the well-known relation

$$r(t) = \frac{\Delta A_{\parallel}(t) - \Delta A_{\perp}(t)}{\Delta A_{\parallel}(t) + 2\Delta A_{\perp}(t)} \quad (1)$$

where $\Delta A_{\parallel}(t)$ and $\Delta A_{\perp}(t)$ are the transient absorbances of the corrected kinetics with parallel and perpendicular polarizations, respectively. The anisotropy decay was then fitted using a deconvolution program, taking the autocorrelation function as the response function. Applying this method, we found that the anisotropy decay determined at 790, 800, and 810 nm and room temperature could be fitted well with a single exponential decay. For example, Figure 5 shows the anisotropic kinetics at 790 and 800 nm together with the best fits. The anisotropy lifetimes are obviously wavelength dependent and were found to be 400 fs at 790 nm, 820 fs at 800, and 360 fs at 810 nm as shown in Table 2. The corresponding initial anisotropies are independent of wavelength; a value of ∼0.4 was found at these

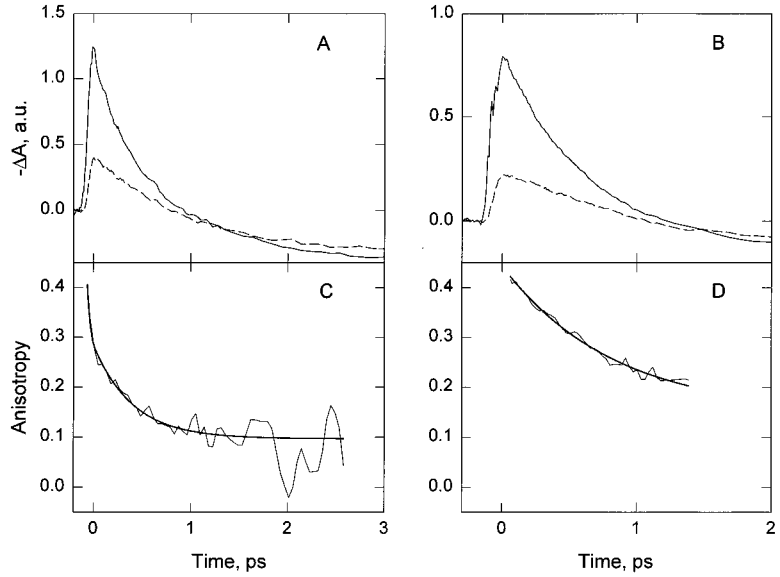


**Figure 5.** Decay kinetics measured at 790 nm (A) and 800 nm (B) and at room temperature with parallel (solid curves) and perpendicular (dashed curves) polarizations. The corresponding anisotropy decays (thin line) and their best fits (thick line) are shown in (C) and (D).

**TABLE 2: Summary of Anisotropy Decay Lifetimes and Initial and Residual Values Obtained by the Optimized Deconvolution Fitting for the Depolarization Kinetics of BChl *a* Molecules in B800−850 Complex from *Rps. acidophila* Measured at Room Temperature and at 77 K[a]**

| $\lambda$ (nm) | $T$ (K) | $\tau$ (fs) | $r$ (0) | $r$ (∞) | $r_L$ (∞) | $r_H$ (∞) |
|---|---|---|---|---|---|---|
| 790 | RT | 400 | 0.40 | 0.10 | 0.03 | 0.13 |
| 800 | RT | 822 | 0.41 | 0.21 | −0.12 | 0.21 |
| 810 | RT | 360 | 0.40 | 0.11 | 0.04 | 0.06 |
| 801 | 77 | 240 | 0.40 | 0.21 | | |

[a] The long time anisotropy values under high and low (without correction for ESA) pump intensities, denoted as $r_H(\infty)$ and $r_L(\infty)$, are listed in the right two columns.

wavelengths. However, the residual values of the anisotropy do change with the wavelength, being higher (0.21) at the central wavelength than at the blue and red edges (0.10−0.11) of the B800 band. It should be pointed out that these anisotropy decay lifetimes obtained at room temperature are in general faster than those obtained for the B800 band of the LH2 preparations from *Rb. sphaeroides* and *Rps. palustris*, as well as from the B800−820 complex from *Rps. acidophila* (strain 7750) also determined by femtosecond transient absorption experiments at room temperature.[6,17]

At 77 K, the anisotropy kinetics at 801 nm calculated by the same method exhibit a faster decay than that observed at room temperature, with the identification of a lifetime of about 240 fs by single exponential decay fitting, as shown in Figure 6. The initial anisotropy is about 0.4, and the residual value (0.21) is the same as that observed at the corresponding wavelength at room temperature. Anisotropic decays at low temperature that were faster than at room temperature were also found recently in the B800 bands (790 and 800 nm) of the intact chromatophores of *Rb. sphaeroides* and *Rps. palustris* at 77 K.[8] This behavior is also found in the isolated B800−820 complex from *Rps. acidophila* (strain 7750) at similar wavelengths and at 77 K.[17]

The long-lived bleaching or ESA signals, under strong or weak excitation intensities, exhibit clearly different residual anisotropies as shown in Figure 7 for the measurements done at 800 nm and at room temperature. This difference is also seen at 790 and 810 nm, as listed in Table 2 (the right two columns).

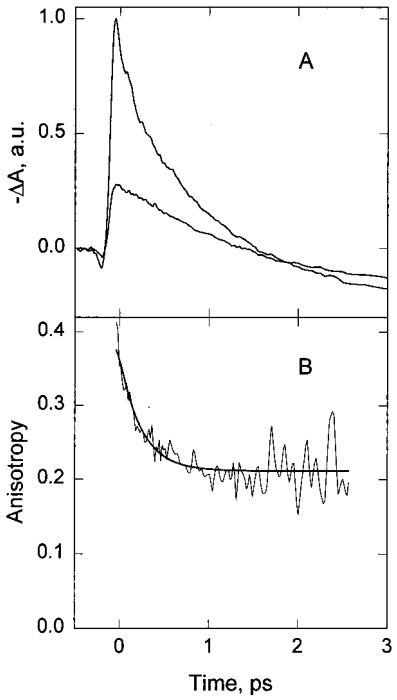


**Figure 6.** (A) Decay kinetics measured at 801 nm and at 77 K with parallel (upper curve) and perpendicular (lower curve) polarizations. (B) Anisotropy decay (thin line) and its best fit (thick line) with a single anisotropy decay time of 0.24 ps.

## IV. Discussion

**A. Intra-B800 Band Energy Transfer**. The depolarization observed within the B800 band indicates energy transfer among the B800 BChl *a* molecules. This transfer was found by previous hole-burning measurements to give ∼930 fs for *Rps. acidophila* and ∼850 fs for *Rb. sphaeroides* at 1.2 K.[15] A faster B800 ↔ B800 transfer time of 0.3−0.4 ps was reported in recent femtosecond transient absorption experiments on the LH2 complexes of *Rb. sphaeroides* and *Rps. palustris* at 77 K.[8] A shorter lifetime of 0.44 ps was additionally found for the transfer from the blue to the red sides of the B800 band in *Rb. sphaeroides*.[22] The depolarization might also be a manifestation of excitonic relaxation. The wavelength dependent depolarization observed in the present work, however, indicates that

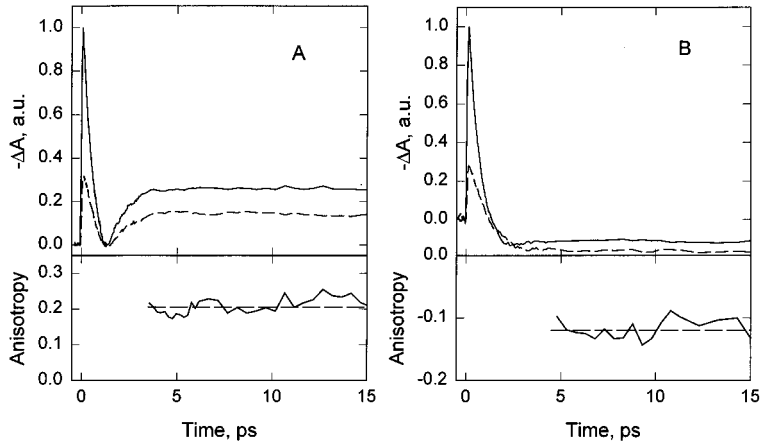


**Figure 7.** Comparison of the long time anisotropy values obtained at 800 nm and at room temperature under strong (A) and weak (B) pump intensities. In each case, the upper panel shows the parallel (solid line) and perpendicular (dashed line) polarized decay kinetics, and the lower panel shows the long time anisotropy (solid lines) calculated directly from the raw data as well as their fits (dashed lines). Note that different scales were used for these two anisotropy plots.

the B800 ↔ B800 transfer or the excitonic relaxation must be wavelength dependent. For the case of an excitonic nature, this wavelength dependence must mean that different excitonic states are involved.

The recent availability of the structural details of the B800 molecules and their spectral properties allows us to calculate the pairwise energy transfer time constant. This calculation was performed by applying the Förster theory in view of the weak coupling due to the relatively large spatial separation of 21.2 Å for Mg···Mg between neighboring B800 BChl *a* molecules. The energy transfer rate depends on the electronic coupling strength between the donor and the acceptor, the mutual orientation of the corresponding transition dipole moments $\kappa$, the spatial separation $R_{ij}$, and the spectral overlap between the donor emission and acceptor absorption spectra. Assuming homogeneously broadened Gaussian profiles for the donor emission and acceptor absorption spectra, the energy transfer rate in $ps^{-1}$ is given by Jean et al.:[23]

$$K_{ij} = \frac{4\pi^2 \times 10^{-24}\kappa^2}{h^2 c n^4 R_{ij}^{\ 6}}\left(\frac{\mu_i^{\ 2}\mu_j^{\ 2}}{2\sqrt{\pi}\sigma_i\sigma_j}\right)\left(\frac{1}{2\sigma_i^{\ 2}}+\frac{1}{2\sigma_j^{\ 2}}\right)^{-1/2} \times \exp\left[\frac{-\Delta^2}{4\sigma_i^{\ 2}\sigma_j^{\ 2}}\left(\frac{1}{2\sigma_i^{\ 2}}+\frac{1}{2\sigma_j^{\ 2}}\right)^{-1}\right] \quad (2)$$

where $n$ is the refractive index of the medium, $\mu_i^2$ and $\mu_j^2$ are the transition dipole strengths of the donor and acceptor, respectively, $h$ is Planck's constant, $c$ is the velocity of light, $\sigma_i$ and $\sigma_j$ are the spectral bandwidths (fwhm) of the donor and acceptor spectra divided by a factor of $(8 \ln 2)^{1/2}$, and the difference between the maxima of these two bands is denoted by $\Delta$. The parameters used for the calculation are 77.5 $cm^{-1}$ for $\Delta$ (calculated using the maxima of the B800 absorption and fluorescence emission bands as shown in Figure 1), 2.12 nm for $R_{ij}$, and 1.24 for $|\kappa|$, obtained from the structure.[5,24] The homogeneous bandwidth $\sigma_i$ and $\sigma_j$ of the B800 BChl *a* was taken to be 220 $cm^{-1}$ as determined by Joo et al. using a LH2 complex from *Rh. sphaeroides*.[11] A value of 40 $D^2$ was used for the transition dipole strengths $\mu_i^2$ and $\mu_j^2$ of the BChl *a*,[25] and $n$ was taken to be 1.5.[14] These parameters give a pairwise transfer time ($1/K_{ij}$) of 2.45 ps. This value is about 3 times larger than the longest experimental depolarization time of 0.82 ps, observed at 800 nm and room temperature (see Table 2). However, it should be noted that the parameter with the largest uncertainty used in the above calculation is the refractive index, and its variation can considerably change the transfer time according to eq 2. A simple calculation indicates that variation of $n$ from 1.0 to 1.5 will result in a change of the transfer time from about 0.5 to 2.4 ps.

We will end this section with a brief discussion of the faster depolarization of the B800 band at 77 K as compared to room temperature (see Table 2). Since a faster depolarization at low temperature was also found in a few other LH2 complexes,[8,17] it therefore can probably be regarded as a common feature of LH2. The shorter depolarization time at low temperature cannot readily be interpreted within the framework of a localized excitation transfer model because a slower transfer time would be expected as a result of the spectral overlap decrease and an increase in the refractive index. We propose that this faster depolarization probably originates from a completely different dynamic process, excitonic state relaxation at low temperature, instead of excitation hopping at room temperature. Moreover, the faster depolarization may also be a manifestation of the apparent wavelength dependence of the fast isotropic recovery component seen at 77 K (0.7−1.3 ps), in contrast to the results obtained at room temperature (∼0.8 ps). Since both the intra- and interband B800 → B850 energy transfer will contribute to the kinetics observed at the blue side of the B800 band,[15] shorter decay times would be expected as seen experimentally at 788 nm and 77 K, i.e., 0.71 ps, as a result of faster intraband relaxation. It should be pointed out that vibronic transitions may also give additional contributions to this fast isotropic decay component.

**B. Energy Transfer from B800 to B850**. The fast isotropic recovery components resolved within the B800 band are attributed to the energy transfer from B800 to B850. This transfer takes ∼0.80 ps at room temperature and seems to have a very weak wavelength dependence. This value is very similar to the transfer time found in other LH2 complexes,[6,8,10] including the B800−820 complex from *Rps. acidophila* (strain 7750).[17] As the temperature is decreased to 77 K, a slightly longer transfer time of 1.30 ps was obtained at 801 nm. This low-temperature transfer time is in excellent agreement with the 1.26 ps transfer time obtained in a previous pump−probe measurement on the B800−850 complex of *Rps. acidophila* (strain 10050) at 803 nm and at the same temperature.[22] It is also very similar to the transfer time in the LH2 complex of *Rb. sphaeroides* reported in a recent low-intensity pump−probe experiment at 77 K.[16]

The similarity of the interband energy transfer in various LH2 antenna complexes, independent of the spectral separation between the B800 and the long absorbing bands, strongly excludes the transfer mechanism from a vibrationally relaxed monomeric donor (B800) to monomeric acceptor (B850) molecules as suggested previously,[14] since for Förster transfer, significant variation of the rate would be expected as the donor and acceptor spectral overlap changes.[26] Two other models have so far been proposed for this interband transfer. In the first model it was suggested that a vibrational mode (750 $cm^{-1}$) of the acceptor is involved in the energy transfer.[10,12] The second one is an excitonic model, where an excited B800 molecule transfers its energy to an excitonic state of the interacting B850 pigments.[10,27]

The validity of this excitonic model, of course, relies on the electronic coupling strength between the B850 molecules. The dipole−dipole coupling between the B850 BChl *a* molecules can be estimated using the structural data for the B800−850 complex. Taking the dipole strength of 40 $D^2$ for BChl *a* [26] and $\kappa$ factors for the BChl *a* molecules within the same and different protomers as 1.19 and 1.67,[24] respectively, and assuming a dielectric constant of 1.0, the pairwise coupling between the BChl *a* molecules within a protomer is about 340 $cm^{-1}$ and that between the nearest-neighboring BChl *a* molecules in proximal protomers is as large as 380 $cm^{-1}$. Such strong pairwise interactions are considerably larger than the maximal coupling between two BChl *a* molecules found in the FMO-protein (200 $cm^{-1}$) of green sulfur bacteria,[28,29] where excitonic states have been suggested to dominate the spectral and dynamic properties. Therefore, the excitonic model seems to be physically reasonable.

**C. Exciton Annihilation and the Roles of the Higher-Lying Excitonic Levels of the B850 Molecular Ring**. The dramatic pump intensity dependence of the transient absorption kinetics observed within the B800 band at room temperature is an interesting new observation. We believed that this is a clear manifestation of the presence of exciton annihilation in the complex. As indicated in section II, there would be more than one B800 molecule per ring (on average, ∼1.4 excitations per B800 ring) being excited under the strongest pump intensity. The rapid interband energy transfer will thus induce a population of more than one exciton per B850 ring and therefore cause exciton annihilation. It is also clear from Figure 2 that this annihilation does occur after the energy transfer from the B800 to the B850 band has occurred, and thus, the possibility that the B800 molecules are involved in this process can be ruled out. The time constant for this annihilation is about 1 ps, corresponding to the depletion of transient absorption at later times ("rise") for the kinetics observed under high pump intensities (Figure 2). It is also consistent with the singlet−singlet annihilation time observed in the LH2 complex of *Rb. sphaeroides* at room temperature using fluorescence up-conversion, where a pulse energy of 0.4 nJ has been used.[27]

Physically, there might be two possibilities for the change of shape of the kinetics, and both of them are related to excessive energy produced by the exciton annihilation process. We first consider the simplest interpretation by assuming that both the B800 and B850 molecules are monomeric in view of the existing interband energy transfer model. Under high excitation intensity, the rapid energy transfer from the B800 to the B850 band (see the insert in Figure 2) might result in the latter being highly populated at a level of more than one excitation per domain. In this case, excitation annihilation can occur according to

$$\mathrm{B850^*} + \mathrm{B850^*} \rightarrow \mathrm{B850^*} + \mathrm{heat} \qquad (3)$$

Excessive energy produced during this annihilation will cause local heating, and at least part of this energy may be converted into excess vibrational energy of the ground and excited states. As a result of the higher vibrational levels being populated, both the GSA and ESA spectra would be either blue- or red-shifted. The magnitude of this spectral shift depends on the energy of the vibrational levels that are populated by the excess energy produced during annihilation. The more energy that is converted, the higher the vibrational levels that can be accessed. Therefore, a gradual spectral shift of the GSA and ESA may be expected. Thus, the observed transient signal at long time may change from ESA under low pump intensity to photobleaching under higher pump intensity.

The alternative model is related to the excitonic energy levels formed by the strong electronic coupling between the B850 molecules, as mentioned in the preceding section. The excitonic energy level scheme for a circular arrangement with one molecule per unit cell has been discussed by Novoderezhkin et al.[30] and Fidder et al.[31] The B850 ring, however, is composed of nine symmetry equivalent protomers, and each contains two BChl *a* molecules. Considering only the nearest-neighbor interactions, the Hamiltonian of the electronic excitation can be expressed as

$$H = \sum_{n=1}^{2N} \Delta E P_n^+ P_n + \sum_{n=n'=1}^{N} M_1 (P_n^+ P_{n'} + P_{n'}^+ P_n) + \sum_{n=n'=1}^{N-1} M_2 (P_{n'}^+ P_{n+1} + P_{n+1}^+ P_{n'}) + M_2 (P_{N'}^+ P_1 + P_1^+ P_{N'}) \qquad (4)$$

where $M_1$ and $M_2$ represent the interactions between the BChl *a* molecules within the same and different protomers, respectively. $\Delta E$ is the excitation energy of the first excited singlet state of an isolated BChl *a* molecule, $N$ is the number of protomers (unit cell) of the B850 ring and it equals 9, according to the crystal structure, $P_n^+$ and $P_n$ are the Pauli creation and destruction operators of the $n$th molecule, and $n$ and $n'$ denote the two BChl *a* molecules in the $n$th protomer. Diagonalization of eq 4 can be performed by two-step transformations and the energies of the $2N$ excitonic levels are given by the following relation:

$$E_{\pm k} = \Delta E \pm \sqrt{{M_1}^2 + 2M_1 M_2 \cos\frac{2\pi k}{N} + {M_2}^2} \qquad (5)$$

where $k = 0, \pm1, \pm2, ..., \pm8, 9$. By application of the dipole−dipole approximation, $M_1$ and $M_2$ were calculated to be 340 and 380 $cm^{-1}$, respectively, as given in the proceding section. A value of $\Delta E$ for a nonexcitonically red-shifted BChl *a* in photosynthetic systems was taken to be 12 500 $cm^{-1}$ (800 nm).[32] Thus, we can calculate the excitonic energy levels by using eq 5 and the result is given in Figure 8. Among the 18 excitonic levels, only $k = 0$ and 9 are nondegenerate and all the rest are doubly degenerate. This excitonic manifold has a large bandwidth with the highest level located at ∼13 220 $cm^{-1}$ (756.4 nm), whereas the lowest level is found at ∼11 780 $cm^{-1}$ (848.9 nm). The latter value is close to the absorption maximum of the B850 band, even though only the dipole−dipole and nearest-neighbor interactions were considered in our simplified model. Although the energy difference between the highest and lowest excitonic levels is about 1440 $cm^{-1}$, the energy difference between the lowest-lying nondegenerate excitonic level and the next doubly degenerate one, located at 845.8 nm, is only 43.3 $cm^{-1}$.

For the two branches of excitonic levels $\pm k$, the transitions from the ground state are optically allowed or forbidden

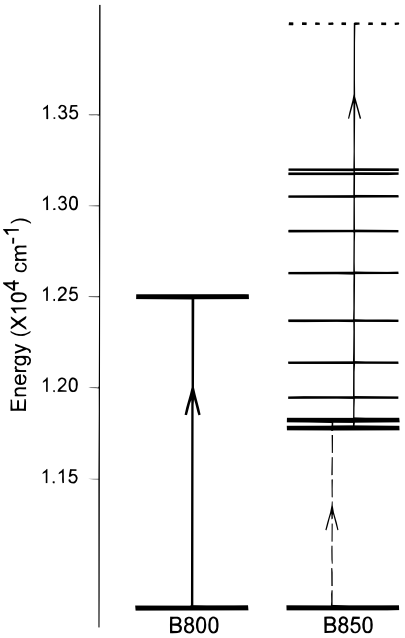


**Figure 8.** Simplified energy level scheme of the B800−850 complex. For B800, only the $S_0$ and $S_1$ states are shown. For B850, the thick horizontal lines represent the lowest-lying excitonic levels of which the lower is nondegenerate and the higher one is doubly degenerate. Variation of the population distribution between these states, because of exciton annihilation, is proposed to be the origin of the observed intensity dependence. The thin horizontal lines denote the higher-lying excitonic levels. The energy levels of the two exciton state and the ground state were placed arbitrarily for clarity. The transitions that correspond to the photobleaching or ESA in the long-lived transient absorption kinetics are indicated by the vertical dashed and solid lines, respectively.

depending not only on the general orientation of the transition dipole moments, in-plane or out-of-plane of the molecular ring, but also on the local geometry of the transition dipole moments for the two BChl *a* molecules within the same protomer. In view of the strong CD signal observed for the B850 band, we believe that the transition dipoles of the B850 BChl *a* molecules in solution are not oriented completely within the ring plane. Thus, transitions to the excitonic states with $k = 0$ as well as $k = -1$ and $-8$ (doubly degenerate) or/and $k = 9$ as well as $k = 1$ and 8 (doubly degenerate) might be optically allowed. For dipole moments oriented close to in-plane, the states with $k = \pm 1$ and $\pm 8$ may carry considerable dipole strength. However, the close antiparallel Qy transition dipoles of the two BChl *a* molecules within the same protomer result in only the lower-lying doubly degenerate excitonic states ($k = -1$ and $-8$) containing much larger dipole strengths. If the diagonal energy disorder, as observed in hole-burning experiments,[12,13] is taken into account, the degeneracy of the excitonic levels would be removed and the transitions to the higher-lying excitonic states can become optically allowed.[33] In this case, the energy difference between the highest and lowest excitonic levels of one branch is ∼590 cm$^{-1}$, which is close to the experimentally determined exciton bandwidth of 600 cm$^{-1}$.[13]

Even in the ideal case, when no diagonal energy disorder is considered, our calculation shows that there are excitonic levels located at 12 862, 12 631, 12 369, and 12 138 cm$^{-1}$, corresponding to 777.5, 791.7, 808.5, and 823.8 nm, respectively, that can act as excellent acceptors for the energy transferred from B800. Relaxation between the excitonic states may proceed very rapidly. The depolarization in the B850 band of the *Rb. sphaeroides* at room temperature was found to be 130 fs by pump−probe experiments[34] and 50−90 fs by fluorescence up-conversion measurements,[27] which is most probably induced by excitonic relaxation processes. Very similar fast decays were also observed within the B820 band in the B800−820 complex of *Rps. acidophila*.[17] The fast isotropic decay component with a lifetime of ∼0.57 ps obtained at 838 nm, where the blue edge of the B850 band is predominantly excited, might also be a manifestation of excitonic relaxation. This fast relaxation will result in the lowest-lying exciton level to be populated. When the pump intensity is high enough, population accumulation at this lowest-lying level would induce exciton annihilation. The conversion of the excessive energy into vibrational energy can change the population distribution between the lowest-lying and its next higher-lying doubly degenerate exciton levels, since it may result in the latter being accessible. Depending on this population distribution as the result of annihilation, the transition absorption would accordingly change with the excitation intensity, since the transition from these higher exciton levels to the two-exciton state may have a red-shifted excited state absorption. The long-lived excess bleaching, observed under stronger pump intensities, most probably represents the thermalized population distribution between the lowest- and its higher-lying exciton states, which decays very slowly, since no further energy acceptor exists. When a low excitation intensity used, a long-lived ESA signal would appear instead, as normally observed (refs 6−8 and 16 and also this work), since only the lowest excitonic state is populated.

To identify the dominant mechanism, the constant anisotropy value at long time offers a nice criterion. Since for the monomeric BChl *a* the polarization of its ESA is essentially parallel to that of its photobleaching and stimulated emission,[35] the long time anisotropy should thus be the same under strong and weak excitation intensity conditions in the case of the vibrational model. However, this is apparently not the case for the excitonic model. Since the population distribution between excitonic levels with different polarizations is different under strong and weak pump intensities, the long time anisotropies under these conditions should accordingly change. As shown in Figure 7, the long time anisotropy values at 800 nm under strong and weak pump intensities are clearly different from each other, 0.21 and −0.12, respectively. These differences are also seen at 790 and 810 nm as shown in Table 2 (the two right columns). This shows that the excitonic model is more likely. We want to point out that a somewhat similar variation of the transient absorption kinetics with excitation intensity has previously been observed in J aggregates of pseudoisocyanine (PIC), where the involvement of densely spaced excitonic states was proposed.[36]

The presence of excitonic states with considerably different energies for the B850 ring has a physical significance for the interband energy transfer. That is a considerable increase in the spectral overlap between the B800 and B850 bands (because of the presence of several higher-lying excitonic levels), and therefore, very rapid interband excitation energy transfer is possible. Even in the case of a spectral shift of the longer-absorbing band, the abundant excitonic states may still maintain an effective spectral overlap (by either the higher- or lower-lying excitonic levels). Moreover, the small oscillator strength carried by those excitonic states, which may serve as energy acceptors for the interband transfer, may not limit the rapid energy transfer. This could be understood by comparing to the vibrational acceptor model. The energy transfer rate in this case depends on the size of the dipole−dipole coupling matrix element and the thermally averaged Franck−Condon factor that is given by the overlap of the initial- and final-state vibrational wave functions. Although several weak vibronic transition

modes between ∼300 and 1300 $cm^{-1}$ may be involved in the interband energy transfer, all these modes have very small Franck−Condon factors, no larger than ∼0.05.[37] This excitonic mechanism of energy transfer is also strongly supported by the recent structural information obtained for the B800−850 antenna complex with the identification of the spatially close arrangement of the B850 molecules.[5] It is also supported by recent femtosecond experiments of spectrally resolved absorbance difference spectroscopy on the isolated B800−850 complexes from *Chromatium tepidum*[10] and from *Rps. acidophila* strain 10050 [Gillbro et al., unpublished observations], where the amplitudes of the absorbance changes of the B850 were observed to be several times larger than that of the B800, the result of the oscillator strength of B850 being concentrated on only a few excitonic states.

## V. Concluding Remarks

The crystal structure of the B800−850 complex of *Rps. acidophila* (strain 10050) reveals the presence of two parallel molecular rings of $C_9$ symmetry[5] comprising different numbers of molecules and especially very different coupling strengths between them. Excitation energy transfer from the B800 to the B850 band was found in the present work to take ∼0.80 ps at room temperature and ∼1.30 ps at 77 K. Depolarization within the B800 band was found to be clearly wavelength dependent at room temperature, and the lifetimes are 400 fs at 790 nm, 820 fs at 800 nm, and 360 fs at 810 nm. This indicates a wavelength dependent excitation hopping or excitonic relaxation within the B800 ring. The even faster depolarization lifetime of ∼0.24 ps observed at 77 K, however, was proposed to be of an excitonic nature.

The observation of pump intensity dependent transient absorption kinetics within the B800 band is of significance in understanding the physical mechanism of energy transfer. The dramatic change of the kinetics under high pump intensity observed within the B800 band, following the transfer from B800 to B850 and the relaxation within the excitonic manifold of the B850, is proposed to be due to the variation of the population distribution between the lowest- and the next higher-lying excitonic levels as a result of exciton annihilation in the lowest excitonic state of the B850. Moreover, the higher-lying excitonic states of the B850 ring can serve as excellent acceptors for the energy transfer from the B800 to the B850 band as the result of improvement of the spectral overlap, and therefore allows very efficient transfer to the B850 ring.

**Acknowledgment.** This research was supported by the Swedish Natural Science Research Council, the British Research Council, and the Human Science Frontiers Program. We thank Dr. A. N. Macpherson for a critical reading of the manuscript. Y.-Z. Ma also thanks the Kempe Foundation for financial support.

## References and Notes

(1) van Grondelle, R.; Dekker, J. P.; Gillbro, T.; Sundström, V. *Biochim. Biophys. Acta* **1994**, *1187*, 1−65.

(2) van Grondelle, R. *Biochim. Biophys. Acta* **1985**, *811*, 147−195.

(3) Hawthornthwaite, A. M.; Cogdell, R. J. In *Chlorophylls*; Scheer, H., Ed.; CRC Press: Boca Raton, FL, 1991; pp 493−528.

(4) Gardiner, A. T.; Cogdell, R. J.; Takaichi, S. *Photosynth. Res.* **1993**, *38*, 159−167.

(5) McDermott, G.; Prince, S. M.; Freer, A. A.; Hawthornthwaite-Lawless, A. M.; Papiz, M. Z.; Cogdell, R. J.; Isaacs, N. W. *Nature* **1995**, *374*, 517−521.

(6) Hess, S.; Feldchtein, F.; Babin, A.; Nurgaleev, I.; Pullerits, T.; Sergeev, A.; Sundström, V. *Chem. Phys. Lett.* **1993**, *216*, 247−257.

(7) Hess, S.; Visscher, K. J.; Pullerits, T.; Sundström, V. *Biochemistry* **1994**, *33*, 8300−8305.

(8) Hess, S.; Åkesson, E.; Cogdell, R. J.; Pullerits, T.; Sundström, V. *Biophys. J.* **1995**, *69*, 2211−2225.

(9) Visscher, K. J.; Gulbinas, V.; Cogdell, R. J.; van Grondelle, R.; Sundström, V. In *Ultrafast Phenomena VIII*; Martin, J.-L., Migus, A., Mourou, G. A., Zewail, A. H., Eds.; Springer Series in Chemical Physics 55; Springer: Berlin, 1993; pp 559−561.

(10) Kennis, J. T. M.; Streltsov, A. M.; Aartsma, T. J.; Nozawa, T.; Amesz, J. *J. Phys. Chem.* **1996**, *100*, 2438−2442.

(11) Joo, T.; Jia, Y.; Yu, J.-Y.; Jonas, D. M.; Fleming, G. R. *J. Phys. Chem.* **1996**, *100*, 2399−2409.

(12) Reddy, N. R. S.; Small, G. J.; Seibert, M; Picorel, R. *Chem. Phys. Lett.* **1991**, *181*, 391−399.

(13) Reddy, N. R. S.; Cogdell, R. J.; Zhao, L.; Small, G. J. *Photochem. Photobiol.* **1993**, *57*, 35−39.

(14) van der Laan, H.; De. Caro, C.; Schmidt, Th.; Visschers, R. W.; van Grondelle, R.; Fowler, G. J. S.; Hunter, C. N.; Völker, S. *Chem. Phys. Lett.* **1993**, *212*, 569−580.

(15) De Caro, C.; Visschers, R. W.; van Grondelle, R.; Völker, S. *J. Phys. Chem.* **1994**, *98*, 10584−10590.

(16) Monshouwer, R.; van Mourik, F.; van Grondelle, R. *Chem. Phys. Lett.* **1995**, *246*, 341−346.

(17) Ma, Y.-Z.; Cogdell, R. J.; Gillbro, T. *J. Phys. Chem.*, submitted.

(18) Cogdell, R. J.; Hawthornthwaite, A. M. In *The Photosynthetic Reaction Center*; Deisenhofer, J., Norris, J. R., Eds,; Academic Press: San Diego, 1993; Vol. 1, pp 23−42.

(19) Clayton, R. K.; Clayton, B. J. *Proc. Natl. Acad. Sci. U.S.A.* **1981**, *78*, 5583−5587.

(20) Ma, Y.-Z.; Feldchtein, F.; Korytin, A. I.; Kiselev, A. M.; Miller, M.; Gillbro, T. *Braz. J. Phys.* **1996**, *26*, 530−542.

(21) Gillbro, T.; Sandström, Å.; Spangfort, M.; Sundström, V.; van Grondelle, R. *Biochim. Biophys. Acta* **1988**, *934*, 369−374.

(22) Monshouwer, R.; Ortiz de Zarate, I.; van Mourik, F.; Picorel, R.; Cogdell, R. J.; van Grondelle, R. In *Photosynthesis: from Light to Biosphere*; Mathis, P., Ed.; Kluwer Academic Publishers: Dordrecht, 1995; Vol. 1, p 91−94.

(23) Jean, J.; Chan, C. K.; Fleming, G. R. *Isr. J. Chem.* **1988**, *28*, 169−175.

(24) Freer, A.; Prince, S.; Sauer, K.; Papiz, M.; Hawthornthwaite-Lawless, A.; McDermott, G.; Cogdell, R. J.; Isaacs, N. *Structure* **1996**, *15*, 449−462.

(25) Pearlstein, R. M. In *Chlorophylls*; Scheer, H., Ed.; CRC Press: Boca Raton, FL, 1991; p 1047.

(26) Förster, Th. *Ann. Phys. (Leipzig)* **1948**, *2*, 55−75.

(27) Jimenez, R.; Dikshit, S. N.; Bradforth, S. E.; Fleming, G. R. *J. Phys. Chem.* **1996**, *100*, 6825−6834.

(28) Tronrud, D. E.; Schmid, M. F.; Matthews, B. W. *J. Mol. Biol.* **1986**, *188*, 433−454.

(29) Pearlstein, R. M. In *Photosynthetic Light-Harvesting Systems*; Scheer, H., Schneider, S., Eds.; De Gruyter: Berlin, 1988; p 555.

(30) Novoderezhkin, V. I.; Razjivin, A. P. *Biophys. J.* **1995**, *68*, 1089−1100. Novoderezhkin, V. I.; Razjivin, A. P. *Photosynth. Res.* **1994**, *42*, 9−15.

(31) Fidder, H.; Knoester, J.; Wiersma, D. A. *J. Chem. Phys.* **1991**, *95*, 7880−7890.

(32) Cogdell, R. J.; Scheer, H. *Photochem. Photobiol.* **1985**, *42*, 669−678.

(33) Reddy, N. R. S.; Picorel, R.; Small, G. J. *J. Phys. Chem.* **1992**, *96*, 6458−6464.

(34) Pullerits, T.; Chachisvilis, M.; Sundström, V. In *Photosynthesis: from Light to Biosphere*; Mathis, P., Ed.; Kluwer Academic Publishers: Dordrecht, 1995; Vol. 1, pp 107−110.

(35) Savikhin, S.; Struve, W. S. *Biophys. J.* **1994**, *67*, 2002−2007.

(36) Sundström, V.; Gillbro, T.; Gadonas, R. A.; Piskarskas, A. *J. Chem. Phys.* **1988**, *89*, 2754−2762.

(37) Wu, H.-M.; Savikhin, S.; Reddy, N. R. S.; Jankowiak, R.; Cogdell, R. J.; Struve, W. S.; Small, G. J. *J. Phys. Chem.* **1996**, *100*, 12022−12033.